

Qualitative Potential Energy Surfaces. 3. Stereoselection Rules for Spin Inversion in Triplet Photochemical Reactions

S. Shaik* and N. D. Epitotis

Contribution from the Department of Chemistry, University of Washington,
Seattle, Washington 98195. Received January 13, 1977

Abstract: The LCFC approach, with inclusion of spin-orbit coupling parts in the effective one-electron Hamiltonian operator, has been used to formulate mechanisms of spin inversion in triplet photoreactions and stereoselection rules for radiationless decay of triplet complexes to singlet ground state products. It is suggested that $\pi\pi^*$ triplet photoreaction complexes can be classified according to the number and direction of atomic orbital rotations required to maximize intermolecular spin-orbit coupling and simultaneously maintain intermolecular bonding. Three classes of triplet photoreaction complexes can be distinguished: (a) Photoaromatic reaction complexes, e.g., $[2\pi_s + 2\pi_s]$, can undergo efficient radiationless decay to ground product if an endomolecular disrotation (ED) accompanied by a simultaneous translational motion is performed. (b) Photoantiaromatic reaction complexes, e.g., $[4\pi_s + 2\pi_s]$, can undergo radiationless decay to ground product if an endomolecular conrotation (EC) accompanied by a simultaneous translational motion is performed. It is argued that monorotational and pyramidalization mechanisms can compete with the ED and the EC mechanisms. The relative importance of the spin inversion mechanism depends on the reaction polarity. (c) Photononaromatic reaction complexes can undergo radiationless decay to ground product if an orthogonal AO pair is generated at the reaction union site.

I. Introduction

In the previous paper,¹ we have shown that the linear combination of fragment configurations (LCFC) method can be utilized to construct qualitative potential energy (PE) surfaces. Applications to the problem of thermal cycloaddition,² which constitute a general model for a thermal reaction, were discussed.

Before attempting to understand the mechanism(s) of photoreactions on the basis of the qualitative PE surfaces generated by the LCFC method, certain crucial time-dependent problems encountered in such reactions must be solved. The mechanism of spin inversion is a problem of this type. In this paper, we suggest a set of selection rules for efficient triplet \rightarrow singlet conversions, by far the most common spin inversion process encountered in organic photochemistry.

II. Theory

In general we can differentiate three classes of photochemical reactions:

(a) Nonionic photoaromatic reactions. This class includes $4n$ electron Hückel photoaromatic reactions (e.g., $[2\pi_s + 2\pi_s]$ cycloadditions) and $4n + 2$ electron Möbius photoaromatic reactions (e.g., $[4\pi_s + 2\pi_a]$ or $[4\pi_a + 2\pi_s]$ cycloadditions). These photoreactions exhibit a manifold of PE surfaces similar to that shown in Figure 1.

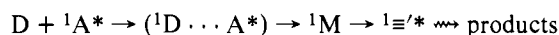
(b) Nonionic photoantiaromatic reactions. This class includes $4n + 2$ electron Hückel photoantiaromatic reactions (e.g., $[4\pi_s + 2\pi_s]$ cycloadditions) and $4n$ electron Möbius photoantiaromatic reactions (e.g., $[2\pi_s + 2\pi_a]$ cycloadditions). These reactions exhibit a manifold of PE surfaces similar to the one shown in Figure 2.

(c) Photononaromatic reactions which involve noncyclic reaction complexes irrespective of the number of electrons. These photoreactions exhibit a manifold of PE surfaces similar to the one shown in Figure 2.

We shall now investigate how the efficiency of spin inversion in triplet photoreactions depends on photoaromaticity, photononaromaticity, and photoantiaromaticity.

A. Triplet Nonionic Photoaromatic Reactions. First, we review the basic features of the model singlet $[2\pi_s + 2\pi_s]$ photocycloaddition which can be described by the following

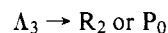
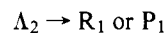
mechanistic scheme.



As the reactants approach each other, a barrier, E^* , is surmounted and an excited intermediate, 1M , is formed. This excited intermediate makes a transition at C_1 to the singlet diexcited surface and is ultimately transformed to the excited intermediate ${}^1\equiv^*$. This, in turn, undergoes fast radiationless conversion to product via the "hole" in the neighborhood of C_2 .^{2,3} (Figure 1).

The efficiency of the ${}^1M \rightarrow {}^1\equiv^*$ transformation depends on the magnitude of the interaction between the boundary of the Λ_2 packet, which contains all the monoexcited diabatic surfaces, and the boundary of the Λ_3 packet, which contains all the diexcited diabatic surfaces (Figure 3). At this point, the reader should recall that the Λ_2 packet boundary defines the singly excited surface for reactants and product, while the Λ_3 packet boundary defines the diexcited surface for reactants which is transformed to the ground surface for product. Furthermore, the Λ_2 - Λ_3 interpacket interaction matrix elements are of the HO-LU type and they vanish in the case of $[2\pi_s + 2\pi_s]$ reactions.² Consequently, any nonsymmetric vibrational motion which removes the symmetry restriction will render the ${}^1\Lambda_2$ - ${}^1\Lambda_3$ surface crossing avoided,⁴ leading to an efficient ${}^1M \rightarrow {}^1\equiv^*$ transformation.

In our subsequent discussions we shall use consistently the notation ${}^{2S+1}\Lambda_n$ to define the crucial state involved in a decay process with the understanding that Λ_n represents a packet boundary and $2S + 1$ the multiplicity of the diabatic surfaces comprising the corresponding packet. The correspondence between this notation and notations referring to the reactant (R) and product (P) states is illustrated below, where R_0 is reactant ground state, R_1 is reactant singly excited state, R_2 is reactant diexcited state, etc.



The LCFC treatment of the triplet $[2\pi_s + 2\pi_s]$ photocycloaddition proceeds in the same manner as that of the corresponding singlet photoreactions, with the singlet diabatic

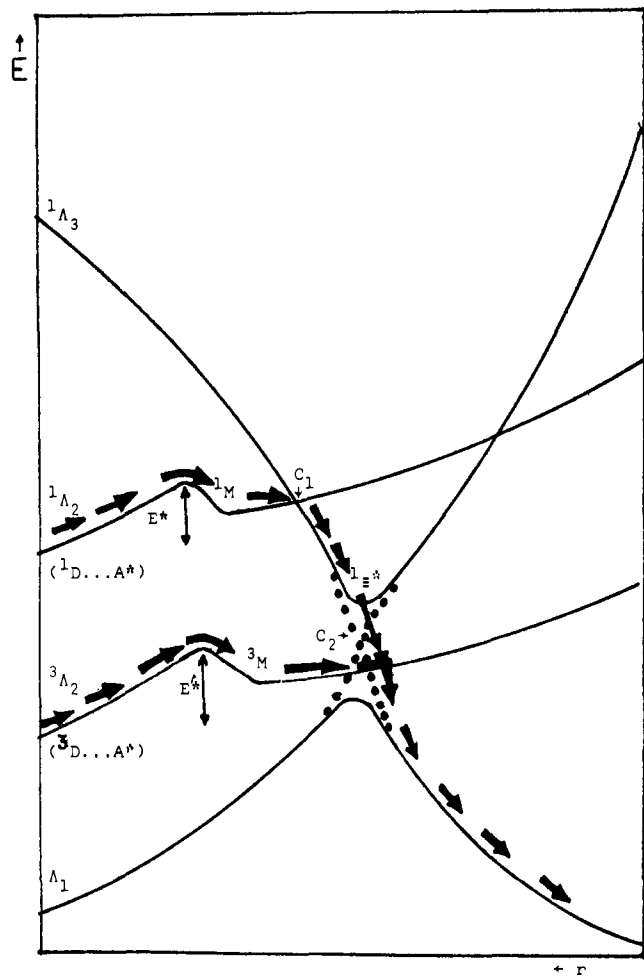
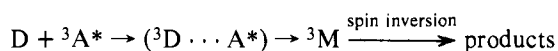


Figure 1. One-dimensional PE surfaces for $[2\pi_s + 2\pi_s]$ cycloaddition reactions. The arrows describe the course of the singlet and the triplet photochemical reactions. Diagram is schematic.

surfaces comprising the Λ_2 packet replaced by their triplet counterparts. The course of the triplet photochemical reaction is described in the following mechanistic scheme:



Qualitatively, this mechanism is similar to the singlet photochemical reaction mechanism with the exception of the spin inversion step. The efficiency of spin inversion is related to the magnitude of the interaction between ${}^3\Lambda_2$ and ${}^1\Lambda_3$ near the "hole". This is, in turn, related to the efficiency of the ${}^3M \rightarrow \text{products}$ transformation.

In order to evaluate the magnitude of the interaction between ${}^3\Lambda_2$ and ${}^1\Lambda_3$ we have to include in the electronic Hamiltonian the appropriate spin-orbit (SO) coupling terms. Accordingly, the ${}^3\Lambda_2$ - ${}^1\Lambda_3$ interaction is expressed by the integral $\langle {}^3\Lambda_2 | \hat{H}_{EI} + \hat{H}_{SO} | {}^1\Lambda_3 \rangle$, where \hat{H}_{EI} is the electronic Hamiltonian and \hat{H}_{SO} is the SO coupling operator. The latter operator can be written as a double sum over the interactions of all electrons, i , with all nuclei, P :

$$\hat{H}_{SO} = \sum_i \sum_P \frac{Z^*_P e^2}{2m^2 c^2} \frac{\hat{l}(i) \cdot \hat{s}(i)}{r_{iP}^3} \quad (1)$$

In this equation, Z^*_P stands for the effective nuclear charge of nucleus P . r_{iP} stands for the distance between electron i and nucleus P , and $\hat{l}(i)$ and $\hat{s}(i)$ are the orbital and spin angular momentum operators for electron i , respectively. Equation 1 can be rewritten as a sum of intra- and intermolecular contributions.

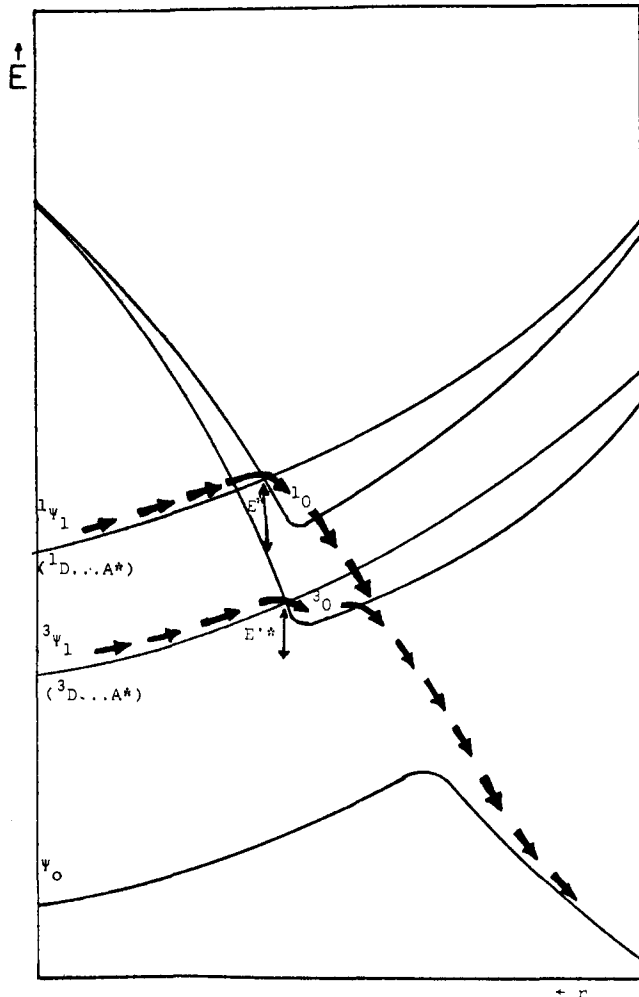


Figure 2. One-dimensional PE surfaces for $[2\pi_s + 2\pi_a]$ cycloaddition reactions. The arrows describe the course of the singlet and the triplet photochemical reactions. Diagram is schematic.

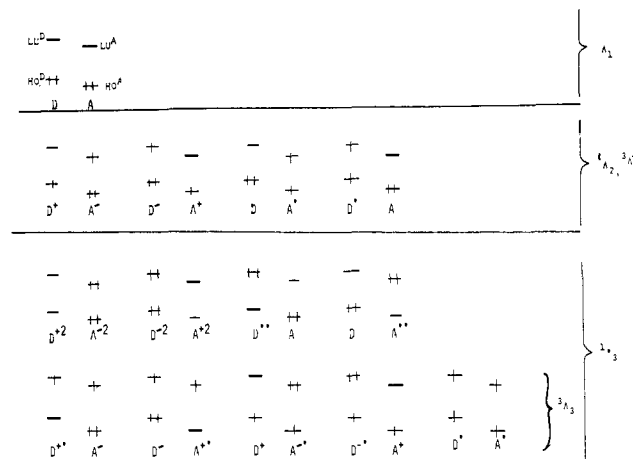


Figure 3. Zero-order configurations and packets for $[\pi + \pi]$ cycloaddition reactions.

$$\hat{H}_{SO} = \hat{H}_{SO}^D + \hat{H}_{SO}^A + \hat{H}_{SO}^{AD} \quad (2)$$

The first two terms of eq 2 describe the intramolecular SO coupling contribution, while \hat{H}_{SO}^{AD} describes the intermolecular contribution. The operators on the right-hand side of eq 2 can be expanded in terms of one-electron operators as

Table I. Effect of Spin Momentum Operators on Atomic Spin Wave Function

Operator	Spin function	
	α	β
\hat{s}_z	$\frac{1}{2} \hbar \alpha$	$-\frac{1}{2} \hbar \beta$
\hat{s}_x	$\frac{1}{2} \hbar \beta$	$\frac{1}{2} \hbar \alpha$
\hat{s}_y	$\frac{i}{2} \hbar \beta$	$-\frac{i}{2} \hbar \alpha$

shown below:

$$\hat{H}_{\text{SO}}^{\text{D}} = \sum_i \hat{h}^{\text{D}}(i) \quad (3)$$

$$\hat{H}_{\text{SO}}^{\text{A}} = \sum_I \hat{h}^{\text{A}}(i) \quad (4)$$

$$\hat{H}_{\text{SO}}^{\text{AD}} = \sum_I \hat{h}^{\text{AD}}(i) \quad (5)$$

The expression for $\hat{h}(i)$ is given by

$$\hat{h}(i) = \sum_P \frac{Z^* p e^2 \hat{l}(i) \cdot \hat{s}(i)}{2m^2 c^2 r_{iP}^3} \quad (6)$$

In our discussions we shall focus attention on SO coupling effected via the intermolecular part of the SO operator since the corresponding interaction matrix element is connected with the stereochemistry of the triplet reaction.

We next consider the forms of the $^3\Lambda_2$ and $^1\Lambda_3$ wave functions. In the case of a nonionic photoaromatic reaction, the $^3\Lambda_2$ wave function is given by

$$^3\Lambda_2 = N[a_1^3(\text{D}^+\text{A}^-) + a_2^3(\text{DA}^*) + a_3^3(\text{D}^*\text{A}) + a_4^3(\text{D}^-\text{A}^+)] \quad (7)$$

In most cases of chemical interest, the lowest charge transfer configuration, $^3\text{D}^+\text{A}^-$, and the lowest locally excited configuration, $^3\text{DA}^*$, make the major contribution. Consequently, we can approximate the $^3\Lambda_2$ wave function as follows:

$$^3\Lambda_2 \simeq N'[a_1'^3(\text{D}^+\text{A}^-) + a_2'^3(\text{DA}^*)] \quad (8)$$

The $^1\Lambda_3$ wave function is given by eq 9 and its approximate form by eq 10.

$$^1\Lambda_3 = M[b_1^1(\text{D}^*\text{A}^*) + b_2^1(\text{D}^+\text{A}^-) + b_3^1(\text{D}^-\text{A}^*) + b_4^1(\text{DA}^{**}) + b_5^1(\text{D}^{**}\text{A}) + b_6^1(\text{D}^-\text{A}^+*) + b_7^1(\text{D}^-\text{A}^+) + b_8^1(\text{D}^+\text{A}^2) + b_9^1(\text{D}^-\text{A}^+2)] \quad (9)$$

$$^1\Lambda_3 = M'[b_1'^1(\text{D}^*\text{A}^*) + b_2'^1(\text{D}^+\text{A}^-) + b_3'^1(\text{D}^-\text{A}^*)] \quad (10)$$

The various monoexcited and diexcited configurations are shown schematically in Figure 3.

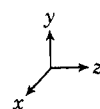
In treating matrix elements, one can make use of two equivalent formulisms, namely, one involving Cartesian operators and real atomic wave functions and another involving ladder operators and complex atomic wave functions.^{5b} We shall make use of the former formulism since it is closely connected with the intuition of the organic chemist. In Cartesian space, the $\hat{l} \cdot \hat{s}$ operator is expanded as shown by

$$\hat{l} \cdot \hat{s} = \hat{l}_x \hat{s}_x + \hat{l}_y \hat{s}_y + \hat{l}_z \hat{s}_z \quad (11)$$

where the \hat{l} components operate only on the orbital parts and the \hat{s} components only on the spin parts of the wave functions. The effect of the \hat{s} operators on spin wave functions and the effect of the \hat{l} operators on atomic spatial wave functions can be gleaned by reference to Tables I and II. In computing matrix elements with respect to the $\hat{l} \cdot \hat{s}$ operator, the following trends

Table II. Effect of Angular Momentum Operators on Cartesian p Atomic Orbitals

Operator	AO		
	p_z	p_x	p_y
\hat{l}_z	0	$i\hbar p_y$	$-i\hbar p_x$
\hat{l}_x	$-i\hbar p_y$	0	$i\hbar p_z$
\hat{l}_y	$i\hbar p_x$	$-i\hbar p_z$	0



revealed by examination of Tables I and II should be kept in mind:

(a) The \hat{s}_z operator leaves the α or β spin wave functions unaltered, i.e., an α or β spin wave function is an eigenfunction of \hat{s}_z . As a result, this operator will render zero any matrix element where the spin parts on the two sides of the operator do not match. By contrast, the \hat{s}_x and \hat{s}_y operators have an opposite effect.

(b) The effect of the \hat{l}_k ($k = x, y, z$) operators on the real wave functions $p_x, p_y,$ or p_z is multiplication by $i\hbar$ or $-i\hbar$ and rotation by 90° about the axis specified by the operator subscript. The three components of the triplet $^3\Lambda_2$ wave function and the single component of the singlet $^1\Lambda_3$ wave function are shown below, where the notation $^{2S+1}M_s\Lambda_2$ and $^{2S+1}M_s\Lambda_3$ are being used.

$$^{3,-1}\Lambda_2 = N'[a_1'^{3,-1}(\text{D}^+\text{A}^-) + a_2'^{3,-1}(\text{DA}^*)]$$

$$^{3,0}\Lambda_2 = N'[a_1'^{3,0}(\text{D}^+\text{A}^-) + a_2'^{3,0}(\text{DA}^*)]$$

$$^{3,1}\Lambda_2 = N'[a_1'^{3,1}(\text{D}^+\text{A}^-) + a_2'^{3,1}(\text{DA}^*)]$$

$$^{1,0}\Lambda_3 = M'[b_1'^{1,0}(\text{D}^*\text{A}^*) + b_2'^{1,0}(\text{D}^+\text{A}^-) + b_3'^{1,0}(\text{D}^-\text{A}^*)]$$

The computed matrix elements^{6,7} are displayed in eq 12-14 and a discussion of the resulting selection rules follows.

$$\begin{aligned} & \langle ^{3,0}\Lambda_2 | \hat{H}_{\text{SO}}^{\text{AD}} | ^{1,0}\Lambda_3 \rangle_z \\ & \simeq \frac{KZ^*}{2\sqrt{2}} \left\{ c_1^{\text{HOA}} c_3^{\text{LUD}} \left\langle p_{1y} \left| \frac{\hat{l}_{z13}}{r^3} \right| p_{3y} \right\rangle \right. \\ & \quad \left. - c_2^{\text{HOA}} c_4^{\text{LUD}} \left\langle p_{2y} \left| \frac{\hat{l}_{z24}}{r^3} \right| p_{4y} \right\rangle \right\} \quad (12) \end{aligned}$$

$$\begin{aligned} & \langle ^{3,\pm 1}\Lambda_2 | \hat{H}_{\text{SO}}^{\text{AD}} | ^{1,0}\Lambda_3 \rangle_x \\ & \simeq \frac{KZ^*}{4} \left\{ c_1^{\text{HOA}} c_3^{\text{LUD}} \left\langle p_{1y} \left| \frac{\hat{l}_{x13}}{r^3} \right| p_{3y} \right\rangle \right. \\ & \quad \left. - c_2^{\text{HOA}} c_4^{\text{LUD}} \left\langle p_{2y} \left| \frac{\hat{l}_{x24}}{r^3} \right| p_{4y} \right\rangle \right\} \quad (13) \end{aligned}$$

$$\begin{aligned} & \langle ^{3,\pm 1}\Lambda_2 | \hat{H}_{\text{SO}}^{\text{AD}} | ^{1,0}\Lambda_3 \rangle_y \\ & \simeq \frac{iKZ^*}{4} \left\{ c_1^{\text{HOA}} c_3^{\text{LUD}} \left\langle p_{1y} \left| \frac{\hat{l}_{y13}}{r^3} \right| p_{3y} \right\rangle \right. \\ & \quad \left. - c_2^{\text{HOA}} c_4^{\text{LUD}} \left\langle p_{2y} \left| \frac{\hat{l}_{y24}}{r^3} \right| p_{4y} \right\rangle \right\} \quad (14) \end{aligned}$$

In the above equations r stands for the intermolecular distance operator and $\hat{l}_{k1,3}$ and $\hat{l}_{k2,4}$ ($k = x, y, z$) are the angular momentum operators which operate only along the reaction union sites and are defined by

$$\hat{l}_{k1,3} = \hat{l}_{k1} + \hat{l}_{k3} \quad (15)$$

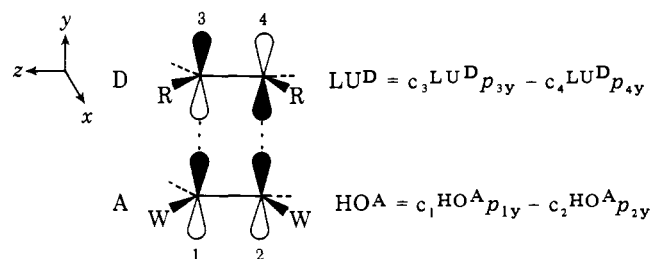
$$\hat{l}_{k2,4} = \hat{l}_{k2} + \hat{l}_{k4} \quad (16)$$

The various indices and symbols can be understood with

Scheme I. Rotational Distortion Motions and Corresponding Complexes for a [${}_2\pi_s + {}_2\pi_s$] Triplet Photocycloaddition (\hat{I}_z Component)

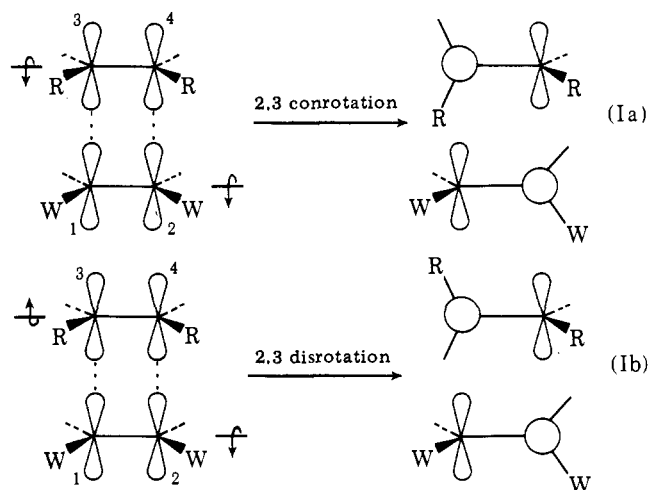
$[{}_2\pi_s + {}_2\pi_s]$ geometry	Nomenclature	Resulting complex	SO efficiency
	Perimolecular conrotation (PC)		Max
	Perimolecular disrotation (PD)		Zero
	Monorotation		Nonzero
	Monorotation		Nonzero
	Endomolecular conrotation (EC)		Zero
	Endomolecular disrotation (ED)		Max

reference to the drawing shown below:



1. \hat{I}_z Selection Rules. Group theoretical considerations indicate that $(\hat{H}_{SO}^{AD})_z$ vanishes in C_s symmetry. Accordingly, efficient SO coupling cannot be effected unless a molecular distortion destroys C_s symmetry and generates orthogonal AOs at the union sites. In the problem at hand, $p_y \rightarrow p_x$ and/or $p_y \rightarrow -p_x$ AO rotations are required. Typical complexes which satisfy the latter condition are shown in Scheme I where the three pairs of complexes differ from each other in terms of the number and direction of AO rotations. By contrast, the two complexes within each pair differ from each other only in terms of the direction of rotations. We now comment on these differences.

First, we compare the Ia and Ib complexes. It can be seen



that while Ia is generated by conrotation of C-2 and C-3, Ib is being generated by a disrotation of the same centers. Similarly, it can be shown that IIIa and IIIb differ also in the sense that IIIa is derived by conrotation of C-3 and C-4, whereas IIIb is generated by disrotation of the same centers. Finally, the partners of pair II are indistinguishable.

Scheme II. Pyramidalization Motions and Corresponding Complexes for a [$2\pi_s + 2\pi_s$] Triplet Photoaromatic Cycloaddition (\hat{l}_x Component)

[$2\pi_s + 2\pi_s$] geometry	Mechanistic type ^a	Resulting complex	SO coupling efficiency
	□ ⁺	(IV)	Nonzero
	□ ⁻	(Va)	Max
	□ ⁻	(Vb)	Zero
	+□ ⁻	(VIa)	Max
	+□ ⁻	(VIb)	Zero
	+□ ⁺	(VIIa)	Max
	-□ ⁺	(VIIb)	Zero
	+□ ⁺	(VIIIa)	Max
	+□ ⁺	(VIIIb)	Zero

Scheme II. (Continued)

$[2\pi_s + 2\pi_s]$ geometry	Mechanistic type ^a	Resulting complex	SO coupling efficiency
		(VIIe)	Nonzero
		(VIIId)	Zero

^a The signs denote the directions of the hybrid AOs, such that a plus (+) sign stands for a hybrid AO pointing downward, and a minus (-) sign stands for a hybrid AO pointing upward.

Members of different pairs involving the same directions of rotation differ in terms of the number and type of AO rotations. Thus, the Ia, Ib, IIIa, and IIIb complexes involve two AO rotations, while the IIa and IIb complexes only one AO rotation. Furthermore, Ia differs from IIIa and Ib differs from IIIb in the sense that the two AO rotations may occur within each reactant (type I complexes) or within one reactant (type III complexes).

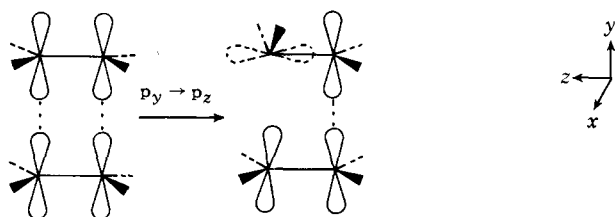
The above discussion leads to the following selection rules:

(a) Spin-orbit coupling is maximized by perimolecular conrotation (PC) or endomolecular disrotation (ED). Both mechanisms are bisrotatory, i.e., they involve two 90° AO rotations.

(b) Spin-orbit coupling is minimized by perimolecular disrotation (PD) or endomolecular conrotation (EC). Both mechanisms are bisrotatory.

(c) Intermediate spin-orbit coupling is produced by a monorotation mechanism.

2. \hat{I}_x Selection Rules. Group theoretical considerations indicate that $(\hat{H}_{SO}^{AD})_x$ vanishes unless a molecular distortion which preserves C_s symmetry and generates orthogonal AOs at the union sites is performed. The necessary AO rotations are $p_y \rightarrow p_z$ and/or $p_y \rightarrow -p_z$, as illustrated below. Clearly, a full 90° rotation is impossible. However, "partial rotation" is possible via pyramidalization of the uniting centers, which mixes π and σ type MOs. A brief background discussion of pyramidalization is presented below.



In a molecule where π - σ separation can be defined, certain distortion modes may effect a mixing of π and σ type MOs. In our case, the distortion mode is pyramidalization. Its net effect is the mixing of $\pi\sigma^*$ and $\sigma\pi^*$ type configurations into ${}^3\Lambda_2$ and ${}^1\Lambda_3$. This, in turn, amounts to mixing of π and σ bonding MOs of the same symmetry as well as π^* and σ^* antibonding MOs of the same symmetry. The degree of σ - π mixing is proportional to the degree of pyramidalization.⁸ Accordingly, we define the new π type MOs after pyramidalization as follows:

$$\pi' = \left(\frac{1}{1 + \lambda_1^2} \right)^{1/2} (\pi^0 + \lambda_1 \sigma) \quad (17)$$

$$\pi'^* = \left(\frac{1}{1 + \lambda_2^2} \right)^{1/2} (\pi^{0*} + \lambda_2 \sigma^*) \quad (18)$$

In the above expressions, π^0 and π^{0*} are the pure π MOs of a planar olefin, π' and π'^* are the new π type MOs after pyramidalization of the olefinic centers, and λ_1 and λ_2 are the pyramidalization coefficients. For a constant pyramidalization, the magnitude of λ_1 or λ_2 depends upon the energy separation and interaction matrix element of the σ^* and π^* (or σ and π) levels⁸ which are admixed by this molecular distortion.

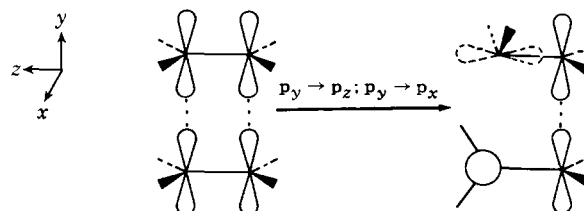
In unraveling the pyramidalization modes which induce SO coupling, we are faced with the problems similar to those encountered in unraveling the rotational modes having the same effect. Specifically, attention should be paid to the number of pyramidalizations as well as the direction thereof. Typical complexes generated by pyramidalization of one or more olefinic centers are displayed in Scheme II. Several trends can be noted:

(a) As the number of pyramidalized centers increases, the absolute magnitude of SO coupling increases. *The pyramidalization mechanism which can best induce SO coupling is that illustrated by complex VIIa.* It involves two pairs of intramolecular bispyramidalizations.

(b) Within a group of complexes involving the same number of pyramidalized centers, one can define a maximally favorable and a minimally favorable pyramidalization mode with intermediate cases becoming possible as appropriate.

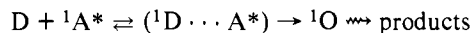
(c) The effectiveness of the pyramidalization mechanism depends on the size of λ .

3. \hat{I}_y Selection Rules. By following similar reasoning as before, we conclude that the critical molecular distortion which can generate efficient SO coupling involves two types of AO rotations, namely, $p_y \rightarrow p_x$ and/or $p_y \rightarrow -p_x$ as well as $p_y \rightarrow p_z$ and/or $p_y \rightarrow -p_z$ as shown below.



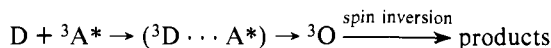
Accordingly, the SO coupling matrix elements with respect to the \hat{I}_y operator give rise to a combination of the rotational and pyramidalization mechanisms already discussed.⁹

B. Triplet Nonionic Photoantiaromatic Reactions. First we review briefly the basic features of a model singlet [$4\pi_s + 2\pi_s$] photocycloaddition on the basis of the qualitative PE surfaces shown in Figure 2. The reaction mechanism can be described by the following chemical equations:



As the reactants approach each other, a barrier, E^* , is surmounted and subsequently, an excited intermediate, 1O , is formed¹⁰ which decays across the energy gap separating ${}^1\Psi_1$ and ${}^1\Psi_0$. Generally, the decay efficiency of such process depends on the energy gap between ${}^1\Psi_1$ and ${}^1\Psi_0$.¹¹ Accordingly, optimization of the radiationless decay process may be achieved by maximizing the ${}^1\Lambda_3-{}^1\Lambda_2$ interpacket interactions ($\text{HO}^D\text{-LU}^A$ and $\text{HO}^A\text{-LU}^D$ type matrix elements) and simultaneously minimizing the ${}^1\Lambda_2-{}^1\Lambda_1$ interpacket interactions ($\text{HO}^D\text{-LU}^A$ and/or $\text{HO}^A\text{-LU}^D$ type matrix elements).² Clearly, these two requirements cannot be met simultaneously and as a result such photoantiaromatic reactions are unfavorable paths owing to the substantial ${}^1\Psi_1-{}^1\Psi_0$ energy gap.

The course of the triplet [$4\pi_s + 2\pi_s$] photocycloaddition can be conveyed by the following chemical equations:¹²



The triplet photoreaction differs from the singlet photoreaction in the following important ways:

(a) Whereas the singlet surface involves an antibonding contribution, due to ${}^1\Lambda_1-{}^1\Lambda_2$ interpacket interactions, the triplet surface involves only bonding contribution. This arises because the ${}^1\Lambda_1-{}^3\Lambda_2$ interaction is zero whereas the ${}^3\Lambda_2-{}^3\Lambda_3$ interactions give rise to bonding along the reaction sites and tend to minimize the photochemical barrier and the ${}^3\Psi_1-{}^1\Psi_0$ energy gap.

(b) The ${}^3\Psi_1 \rightarrow {}^1\Psi_0$ radiationless decay of the triplet [$4\pi_s + 2\pi_s$] complex is accompanied by a spin inversion process.

The wave functions which describe the triplet excited and the ground surfaces are shown below.

$${}^1\Psi_0 = N_0 [a_1^1(\text{DA}) + a_2^1(\text{D}^+\text{A}^-) + a_3^1(\text{D}^-\text{A}^+) + a_4^1(\text{D}^*\text{A}^*) + a_5^1(\text{D}^{**}\text{A}) + a_6^1(\text{DA}^{**}) + a_7^1(\text{D}^{+2}\text{A}^{-2}) + a_8^1(\text{D}^{-2}\text{A}^{+2})] \quad (19)$$

$${}^3\Psi_1 = M_1 [b_1^3(\text{D}^+\text{A}^-) + b_2^3(\text{D}^-\text{A}^+) + b_3^3(\text{D}^*\text{A}^*) + b_4^3(\text{D}^*\text{A}^*)] \quad (20)$$

The approximate wave functions are given below.

$${}^1\Psi_0 \approx N_0' [a_1'^1(\text{DA}) + a_2'^1(\text{D}^+\text{A}^-)] \quad a_1' > a_2' \quad (21)$$

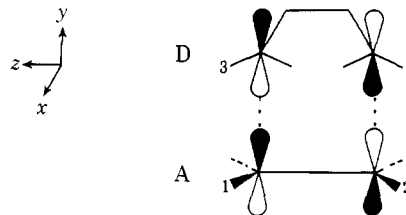
$${}^3\Psi_1 \approx {}^3(\text{D}^+\text{A}^-) \quad (22)$$

The computed matrix elements are shown below and a discussion of the resulting selection rules follows:

$$\langle \hat{H}_{\text{SO}^{\text{AD}}} \rangle_z = \frac{-K_1 Z^*}{\sqrt{2}} \left\{ c_3^{\text{HO}^D} c_1^{\text{LU}^A} \left\langle p_{3y} \left| \frac{\hat{I}_{z13}}{r^3} \right| p_{1y} \right\rangle + c_4^{\text{HO}^D} c_2^{\text{LU}^A} \left\langle p_{4y} \left| \frac{\hat{I}_{z24}}{r^3} \right| p_{2y} \right\rangle \right\} \quad (23)$$

$$\langle \hat{H}_{\text{SO}^{\text{AD}}} \rangle_x = \frac{+K_1 Z^*}{2} \left\{ c_3^{\text{HO}^D} c_1^{\text{LU}^A} \left\langle p_{3y} \left| \frac{\hat{I}_{x13}}{r^3} \right| p_{1y} \right\rangle + c_4^{\text{HO}^D} c_2^{\text{LU}^A} \left\langle p_{4y} \left| \frac{\hat{I}_{x24}}{r^3} \right| p_{2y} \right\rangle \right\} \quad (24)$$

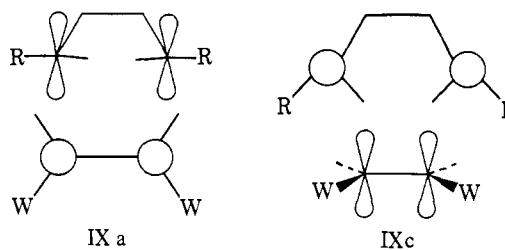
$$\langle \hat{H}_{\text{SO}^{\text{AD}}} \rangle_y = \frac{-iK_1 Z^*}{2} \left\{ c_3^{\text{HO}^D} c_1^{\text{LU}^A} \left\langle p_{3y} \left| \frac{\hat{I}_{y13}}{r^3} \right| p_{1y} \right\rangle + c_4^{\text{HO}^D} c_2^{\text{LU}^A} \left\langle p_{4y} \left| \frac{\hat{I}_{y24}}{r^3} \right| p_{2y} \right\rangle \right\} \quad (25)$$



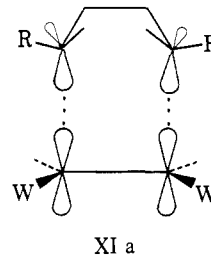
$$\text{HO}^D = c_3^{\text{HO}^D} p_{2y} - c_4^{\text{HO}^D} p_{4y}$$

$$\text{LU}^A = c_1^{\text{LU}^A} p_{1y} - c_2^{\text{LU}^A} p_{2y}$$

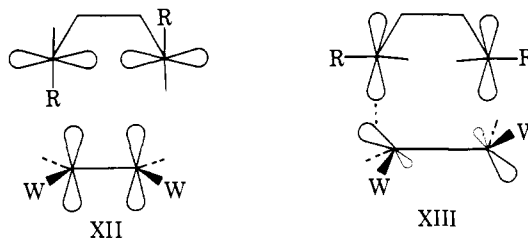
1. \hat{I}_z Selection Rules. Group theoretical considerations indicate that the integrals of eq 23 are maximized by a molecular motion which preserves C_s symmetry and generates orthogonal AOs at the union sites. In the problem at hand, orthogonal x - y AO relationships are required. Typical complexes which satisfy the latter condition are shown in Scheme III. The rotational mechanism involving the lowest energetic price as well as the pyramidalization mechanism which maximizes SO coupling are shown below.



IX a IX c
endomolecular conrotation (EC)



2. \hat{I}_x Selection Rules. Group theoretical considerations indicate that $\langle \hat{H}_{\text{SO}^{\text{AD}}} \rangle_x$ is maximized by a molecular distortion which removes C_s symmetry and generates orthogonal AOs at the union sites. In the problem at hand, orthogonal y - z relationships are required. The rotational and pyramidalization mechanisms which involve maximization of the SO coupling are shown below.



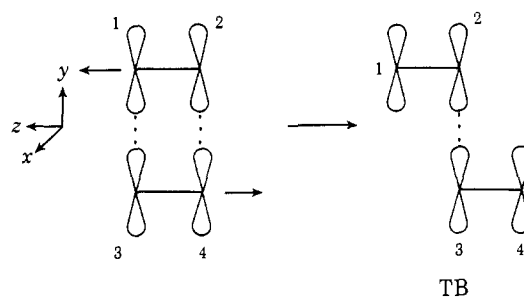
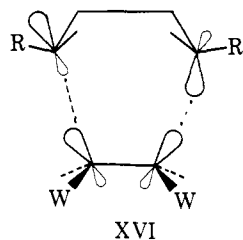
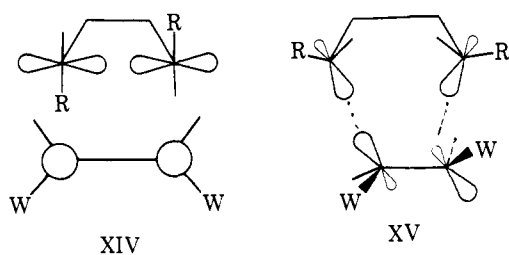
3. \hat{I}_y Selection Rules. By following similar reasoning as before, we conclude that the critical molecular distortion which can generate efficient SO coupling involves $p_y \rightarrow p_x$ and/or $p_y \rightarrow -p_x$ as well as $p_y \rightarrow p_z$ and/or $p_y \rightarrow -p_z$ AO rotations. The distortion mechanisms which maximize the SO coupling and involve the least energetic price are shown below.

C. Weak SO Coupling Mechanisms. In addition to the rotational and pyramidalization mechanisms described above,

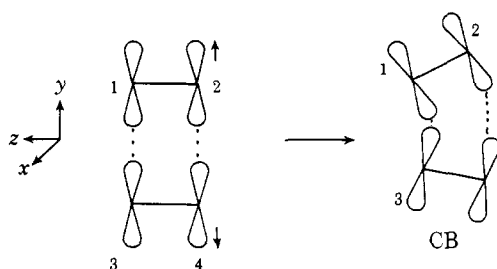
Scheme III. Rotational and Pyramidalization Mechanisms for a $[4\pi_s + 2\pi_s]$ Triplet Photoreaction (\hat{I}_z Component)

$[4\pi_s + 2\pi_s]$ geometry	Nomenclature ^a	Resulting complex	SO efficiency
	Endomolecular conrotation (EC)		Max
	Endomolecular disrotation (ED)		Zero
	Endomolecular conrotation (EC)		Max
	Monorotation		Nonzero
			Max
			Zero

^aFor an explanation of the sign convention, see footnote *a* in Scheme II.



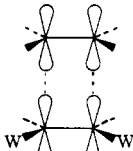
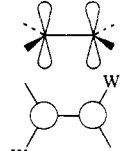
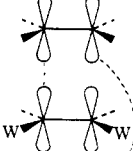
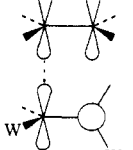
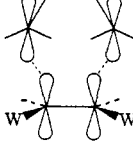
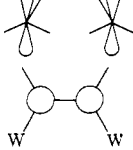
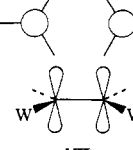
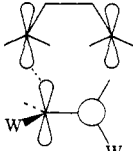
This induces a weak SO coupling interaction which can be intensified by the pyramidalization of the union centers. Another antisymmetric motion along the *y* axis leads to the CB



there can be additional mechanisms which induce SO coupling. A brief discussion is given below.

The SO matrix element $\langle {}^3\Lambda_2 | \hat{H}_{SO} | {}^1\Lambda_3 \rangle$ in the $[2\pi_s + 2\pi_s]$ geometry can have a nonvanishing value if the system performs an antisymmetric vibrational motion. Such a motion along the *z* axis may lead to the TB structure shown below.

Scheme IV. SO Coupling in $[2\pi + 2\pi]$ and $[4\pi + 2\pi]$ Mechanisms

Complex ^a	Nomenclature	SO coupling	Characteristic PE surface manifold	Stereochemical result
	(I) $[2\pi_s + 2\pi_s]$	Zero	Aromatic	
	(II) ED	Max	Diabatic	Isomerization
	(III) Translation rotation (ED)	Max	Antiaromatic	$[2s + 2a]$ addition
	(IV) Monorotation	Nonzero	Nonaromatic	Diradicaloid formation
	(V) $[4\pi_s + 2\pi_s]$	Zero	Antiaromatic	
	(VI) Translation rotation (EC)	Max	Antiaromatic	$[4s + 2s]$ addition
	(VII)			
	(VIII) Monorotation	Nonzero	Nonaromatic	Diradicaloid formation

^a The translation rotation (ED) mechanism is shown formally.

structure which, again, can intensify the SO coupling interaction by pyramidalization of the union centers. This mechanism may be termed the vibronic SO coupling mechanism.

At this point it should be emphasized that the stereoselection rules for efficient SO coupling were based on the assumption that the ${}^3D^+A^-$ crosses the ${}^3DA^*$ (or ${}^3D^*A$) diabatic surface, i.e., the lowest energy diabatic surface of the 3A_2 packet for intermolecular distance of interest is assumed to be ${}^3D^+A^-$. This is the situation which is very frequently encountered in organic triplet photoreactions. However, cases may be found where the relative energy of ${}^3D^+A^-$ and ${}^3DA^*$ (or ${}^3D^*A$) switches around. In such an event the crucial SO coupling matrix elements may, in principle, change and result in different spin inversion mechanisms. However, a careful examination of the relative energetics of diabatic surfaces suggest that in *nearly* all imaginable cases, the crucial SO coupling matrix elements in photoaromatic reactions are of the HO-LU

type regardless of the relative ordering of the lowest charge transfer and lowest locally excited diabatic surfaces. However, in photoantiaromatic reactions where ${}^3DA^*$ or ${}^3D^*A$ lies below ${}^3D^+A^-$ at moderate or short intermolecular distances, the intermolecular SO coupling matrix element is of the HO^D-HO^A or LU^D-LU^A type. In such cases the selection rules will resemble those for photoaromatic reactions.

III. Mechanisms of Triplet Photoreactions

In discussing the mechanisms of different classes of photoreactions (i.e., photoaromatic, etc.), attention should be paid to the fact that, as one or both reactants suffer a geometrical distortion so that the requisite spin inversion process is optimized, the shapes of the adiabatic PE surfaces are simultaneously altered. Accordingly, we must seek a compromise geometry which is consistent with highly, though not maxi-

mally, efficient SO coupling as well as maintenance of bonding between the two reactants. This is a key premise for the subsequent discussions of triplet photoreaction mechanisms and it will be illuminated by reference to Scheme IV.

Consider a triplet photoaromatic reaction where the triplet photoexcited olefin approaches the ground singlet olefin in a $[2\pi_s + 2\pi_s]$ manner (structure I in Scheme IV). Near the “hole”, ED, required for maximal SO coupling, converts structure I to structure II (Scheme IV). This process eliminates intermolecular bonding and simultaneously annihilates the decay “hole” generated by the ${}^1\Lambda_1-{}^1\Lambda_3$ interaction, because all photoaromatic PE surfaces are transformed to diabatic PE surfaces. *The result is decay of the $[2\pi_s + 2\pi_s]$ complex back to ground reactants, one or both of which are isomerized depending on the relative endorotatory efficiency of the olefins.*

An alternative motion which can occur in the neighborhood of the “hole” is ED with a simultaneous translation of the frame of one reactant relative to the other in the manner indicated by structure III (Scheme IV). This results in efficient SO coupling, generation of bonding between the reactants, and simultaneous annihilation of the decay “hole”. This occurs because the mechanism transforms photoaromatic to photoantiaromatic PE surfaces. More specifically, this rotation-translation mechanism results in SO coupling of the ${}^3\Psi_1-{}^1\Psi_0$ (eq 19 and 20) rather than the ${}^3\Lambda_2-{}^1\Lambda_3$ (eq 8 and 10 states, and ${}^3\Psi_1$ as well as ${}^1\Psi_0$ involve pericyclic bonding. The result of these PE transformations is equivalent to decay of the triplet complex to singlet products across an energy gap (Figure 2). In short, SO coupling necessitates the transformation of a triplet photoaromatic to a triplet photoantiaromatic reaction in the translation-rotation (ED) mechanism.

The situation becomes somewhat different when the rotational mechanism generates orthogonal AOs along one pair and nonorthogonal AOs along a second pair of union sites. Once again, consider the $[2\pi_s + 2\pi_s]$ approach of a triplet excited and a ground olefin. In the neighborhood of the “hole” monorotation converts structure I to structure IV (Scheme IV). This process gives rise to efficient, though not maximal, SO coupling. In addition, it preserves intermolecular bonding but destroys the decay “hole” because all photoaromatic surfaces are transformed to nonaromatic PE surfaces. However, back rotation by $\pm 90^\circ$ can regenerate the decay “hole” and lead to efficient product formation. Consequently, the decay aspect of the monorotational mechanism may be superior to that of the ED mechanism.

The rotational mechanisms of the $[4\pi_s + 2\pi_s]$ cycloaddition can be illuminated in a similar manner. The basic conclusions are spelled out in Scheme IV.

Pyramidalization mechanisms stand in contrast to rotational mechanisms in the sense that pyramidalization distortion modes preserve the basic PE surface interrelationships present in the absence of distortion. *Accordingly, although such mechanisms are inferior to the rotational mechanisms insofar as promoting efficient SO coupling, they retain the necessary features, e.g., intermolecular bonding, decay “hole”, etc., for transformation of triplet excited reactants to ground singlet products.*

At this point, it should be noted that the pyramidalization mechanism may become prominent under the following circumstances:

(a) Both reactants contain the π bond constrained within a small ring such that rotations are restricted.

(b) The reactants have low-lying σ^* MOs,⁸ the presence of which may become responsible for inducing pyramidalization of the appropriate reaction sites.

A comparison of the decay processes involved in the ED and the pyramidalization mechanisms of a $[2\pi_s + 2\pi_s]$ triplet photocycloaddition can be made by reference to Figure 4. This

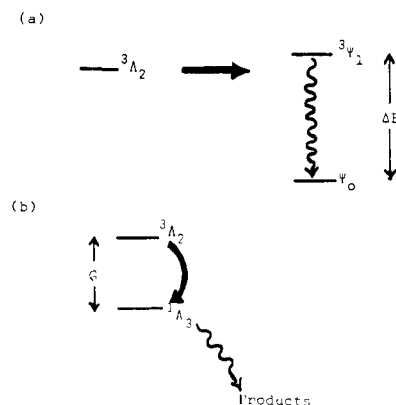


Figure 4. Transformation of PE surface manifold and resulting decay energy gaps. (a) Translation rotational (ED) mechanism. (b) $[2\pi_s + 2\pi_s]$ pyramidalization mechanism.

is an ideogram which depicts the major events involved in the transformation of triplet reactants to singlet products.

The ED mechanism involves a less favorable decay energy gap factor, while the pyramidalization mechanism involves the best decay energy gap factor since the decay “hole” which is preserved by this mechanism separates the upper (${}^3\Lambda_2$) from the lower (${}^1\Lambda_3$) state by only a small gap denoted by G . The “hole” is of the order of $\sim 1-2$ eV¹³ and this is an upper bound for G . Clearly, the ED mechanism will be disfavored relative to the pyramidalization mechanism when ΔE is much larger than G , i.e., decay will be unfavorable due to a large energy gap despite efficient SO coupling. The situation will reverse when $\Delta E \simeq G$. The monorotation mechanism will become important in intermediate cases.

A similar comparison of mechanisms can be made for the case of $[4\pi_s + 2\pi_s]$ photocycloadditions. Here, the EC mechanism will become more prominent as polarity increases.

IV. Discussion

In this work, we have attempted to provide a qualitative theoretical framework for guiding our thinking regarding triplet photoreactions. We have assumed that spin inversion plays a central role in triplet photoreactions and we concentrated on evaluating the chemical implications of the inter- and intramolecular components of the crucial SO coupling matrix element. The major theoretical ideas developed in this work are the following:

(a) A triplet $4n$ electron photoreaction exhibits a dichotomy insofar as the first part of the reaction, i.e., photochemical barrier crossing, is controlled directly by a large one-electron *electronic* matrix element of the HO-HO and/or LU-LU type, while the second part, i.e., spin inversion, is controlled by a one-electron *SO coupling* matrix element of the HO-LU type. These two different interactions dictate different geometries for the reaction complex. *If an ED mechanism for SO coupling is operative, a triplet $4n$ electron photoreaction will be partly photoaromatic (photochemical barrier) and partly photoantiaromatic (decay) with photoantiaromaticity imposed by the necessity of spin inversion. This mechanism will result in products having stereochemistry expected from a photoantiaromatic reaction. If the pyramidalization mechanism is operative, the $4n$ electron photoreaction will be photoaromatic-like throughout.*

(b) A triplet $4n + 2$ electron photoreaction exhibits no dichotomy. In this case, the photochemical barrier is controlled indirectly by a large HO-LU type one-electron *electronic* interaction matrix element. Furthermore, spin inversion is controlled by a one-electron *SO coupling* matrix element also of the HO-LU type. Regardless of whether the rotational or pyramidalization SO coupling mechanisms operate, the

Scheme V. Stereoselectivity of Triplet Photoreactions

No. of electrons	Reactivity spectrum		
	Polar reaction		Nonpolar reaction
$4n$	Predominant $s + a$	Predominant diradicaloid	Predominant $s + s$
$4n + 2$	Predominant $s + s$	Predominant diradicaloid	Predominant $s + a$

product stereochemistry will be that expected from a photoantiaromatic reaction.

(c) Reaction polarity¹⁴ modulates the expression of SO coupling potential. In nonpolar cases, a large decay energy gap renders unfavorable the mechanisms which afford maximum SO coupling efficiency. In such cases, modest SO coupling efficiency complements an optimally small decay energy gap in the case of the pyramidalization mechanism. *In polar cases the energy gap factor ceases to be a problem. In this case, mechanisms affording maximum SO coupling can become dominant.*

The dependence of stereoselectivity on reaction polarity in the case of triplet photoreactions is spelled out in Scheme V. The rules embodied in this scheme are, of course, very approximate, but they can hopefully provide the basis for constructive experimentation.

In addition to the above stereochemical considerations certain other effects peculiar to triplet photoreactions should be noted.

(a) The intermolecular distance effect. The magnitude of SO coupling matrix element is inversely proportional to the internuclear distance. It is clear that, in order to achieve SO coupling interaction, the interacting centers should assume small internuclear distances.

The importance of the distance effect can be illustrated by reference to a photoantiaromatic reaction. In both singlet and triplet cases, the lowest excited surface characteristics can be attributed to the $D^+A^- - D^*A^*$ interaction which is of the $HO^A - LU^D$ type. The resulting surface is having a shallow minimum which contains the O intermediate. A singlet [$4\pi + 2\pi$] photoreaction will involve decay at relatively long intermolecular distances where steric effects are not prohibitive. Hence, such reaction may yield sterically congested products if secondary orbital effects dictate so. By contrast, the triplet reaction will involve decay at shorter intermolecular distance and may yield strain-free products.

(b) The heavy atom effect. The SO coupling matrix element is directly proportional to the atomic number^{5b} of an atom. Hence, whenever a reactant contains a heavy atom center which is not directly involved in the reaction, strong SO coupling may obtain, without any need of distortion, via the agency of the heavy atom, which can provide the needed orthogonal AO interactions.

(c) The MO degeneracy effect. Consider the case where the HO of one reactant is doubly degenerate, the MOs being symbolized by $\phi(0^\circ)$ and $\phi(90^\circ)$ and spanning AOs which are mutually orthogonal. In such a case, one may replace $\phi(0^\circ)$ and $\phi(90^\circ)$ by in-phase and out-of-phase linear combinations. This ensures that the SO coupling matrix element between one or both of these degenerate MOs and the LU of the second reactant can be optimized without the need of rotation or other nuclear distortions.

While we exemplified the key concepts involved by reference to photocycloadditions initiated by triplet $\pi\pi^*$ excitation, the basic conclusions remain unaltered in the case of triplet $\pi\pi^*$ involved photocycloadditions initiated by triplet $n\pi^*$ excitation where DA^* ($n\pi^*$) or D^*A ($n\pi^*$) is crossed by D^+A^- . Once the reaction system finds itself on the adiabatic surface arising primarily from the D^+A^- diabatic surface the crucial SO coupling matrix element involves $HO-LU$ interaction and the

situation resembles the one encountered in triplet $\pi\pi^*$ photocycloadditions. Many triplet $n\pi^*$ photocycloadditions belong to this class. Any polar nonionic triplet photocycloaddition will obey the same rules regardless of the type of excitation.

Finally, in the case of photononaromatic reactions (e.g., bicentric reactions) the mechanism of spin inversion is simple and requires a motion which generates an orthogonal AO pair at the reaction site.

Until recently, theoretical organic chemistry could be aptly described as the study of the matrix elements of the electronic Hamiltonian, which contains no coupling terms. As a result, certain types of chemical problems, where the importance of coupling figures prominently, have remained begging solution. One such problem is the mechanism of chemical reactions which necessitate spin inversion in the course of the transformation of reactants to products. Indeed, a large body of organic chemical reactions involves triplet reactants converted to singlet products.

In recent years, attention has been drawn to the key role of SO coupling in triplet reactions as a result of important experimental studies which demonstrated unexpected facile singlet \rightarrow triplet conversions.¹⁵ The theoretical discussion of SO coupling in simple molecular systems contained in the excellent text by McGlynn et al.^{5b} constitutes ideal background for the organic chemist who seeks to familiarize himself with the quantum mechanics of SO coupling. This work emphasizes the importance of one-center SO coupling in spectroscopic problems. Recent publications by Salem¹⁶ emphasize the potential importance of SO coupling in model reaction systems and draw attention to the two-center SO coupling.

In this paper, we presented a coherent theoretical framework which makes possible a rational approach to triplet reactants. Relatively simple experiments could suggest how the proposed model can be improved or reveal new, before unsuspected, important factors.

Acknowledgment. This work was supported by a NATO Grant (in collaboration with Professor F. Bernardi) and an A. P. Sloan Fellowship (1976-1978) to N.D.E.

References and Notes

- (1) See part 1: N. D. Epiotis and S. Shaik, *J. Am. Chem. Soc.*, accompanying paper in this issue.
- (2) See part 2: N. D. Epiotis and S. Shaik, *J. Am. Chem. Soc.*, accompanying paper in this issue.
- (3) (a) W. Th. A. M. van der Lugt and L. J. Oosterhoff, *J. Am. Chem. Soc.*, **91**, 6042 (1969); (b) J. Michl, *Fortschr. Chem. Forsch.*, **46**, 1 (1974); *Pure Appl. Chem.*, **41**, 507 (1975); (c) W. G. Dauben, L. Salem, and N. J. Turro, *Acc. Chem. Res.*, **8**, 41 (1975).
- (4) For discussions of avoided surface crossing see (a) L. Salem, *J. Am. Chem. Soc.*, **96**, 3486 (1974); (b) L. Salem, C. Leforestier, G. Segal, and R. Wetmore, *J. Am. Chem. Soc.*, **97**, 479 (1975); (c) L. Salem, *Science*, **191**, 882 (1976).
- (5) For a discussion of the approximations involved see (a) S. McClure, *J. Chem. Phys.*, **17**, 665 (1949); (b) S. P. McGlynn, T. Azumi, and M. Kinoshita, "The Triplet State", Prentice-Hall, Englewood Cliffs, N.J., 1969; (c) S. P. McGlynn, L. G. Vanquickenborne, M. Kinoshita, and D. G. Carroll, "Introduction to Applied Quantum Chemistry", Holt, Rinehart and Winston, New York, N.Y., 1972.
- (6) Rules for evaluation of matrix elements between Slater determinants are discussed in W. G. Richards and J. A. Horsley, "Ab Initio Molecular Orbital Calculations for Chemists", Clarendon Press, Oxford, 1970.
- (7) The intramolecular SO coupling operators in eq 2 give rise also to intramolecular matrix elements of the type $HO^D - LU^D$ for the interaction of ${}^3DA^*$ and D^*A^* and intramolecular matrix elements of the type $HO^A - LU^A$ and $HO^D - LU^D$ for the interaction of ${}^3D^+A^-$ and D^+A^- , respectively. These matrix elements are maximized by a monorotation motion (vide infra).
- (8) The problem of pyramidalization is discussed by (a) W. Cherry and N. D. Epiotis, *J. Am. Chem. Soc.*, **98**, 1135 (1976); (b) N. D. Epiotis, W. Cherry, S. Shaik, R. L. Yates, and F. Bernardi, *Top. Curr. Chem.*, **70** (1977).
- (9) A more detailed discussion can be found in S. Shaik, Ph.D. Dissertation, University of Washington, 1978.
- (10) An 'O intermediate is described by a wave function having major charge transfer (D^+A^-) and diexcitation (D^*A^*) contribution.
- (11) Other factors which are neglected in our approach, such as the kinetic energy of the reaction partners, the slopes of diabatic surfaces, and the density of the vibronic levels, are also important. For detailed discussions see (a) C. Zener, *Proc. R. Soc. London, Ser. A*, **137**, 696 (1932); (b) L.

- Landau, *Phys. Z. Sowjetunion*, **2**, 46 (1932); (c) G. W. Robinson and R. P. Frosch, *J. Chem. Phys.*, **37**, 1962 (1962); (d) *ibid.*, **38**, 1187 (1963); (e) J. Jortner, S. A. Rice, and R. M. Hochstrasser, *Adv. Photochem.*, **7**, 149 (1969); (f) J. Jortner, *Pure Appl. Chem.*, **27**, 329 (1971).
- (12) An ^3O intermediate is described by a wave function having major charge transfer ($^3\text{D}^+\text{A}^-$) and diexcitation ($^3\text{D}^*\text{A}^*$) contributions.
- (13) D. Grimbert, G. Segal, and A. Devaquet, *J. Am. Chem. Soc.*, **97**, 6629 (1975).
- (14) The reaction polarity is defined as $(I_D - A_A)^{-1}$, where I_D is the ionization potential of the donor reactant and A_A is the electron affinity of the acceptor

- reactant.
- (15) (a) N. J. Turro and P. Lechtken, *J. Am. Chem. Soc.*, **94**, 2886 (1972); (b) H. C. Steinmetzer, A. Yekta, and N. J. Turro, *ibid.*, **96**, 282 (1974); (c) N. J. Turro, P. Lechtken, G. Schuster, J. Orell, H. C. Steinmetzer, and W. Adam, **97**, 1627 (1975); (d) N. J. Turro and A. Devaquet, *ibid.*, **97**, 3859 (1975); (e) N. J. Turro, V. Ramamurthy, K. C. Liu, A. Krebs, and R. Kemper, *ibid.*, **98**, 6758 (1976); (f) T. R. Darling and C. S. Foote, *ibid.*, **96**, 1625 (1974).
- (16) (a) L. Salem and C. Rowland, *Angew. Chem., Int. Ed. Engl.*, **11**, 92 (1972); (b) L. Salem, *Pure Appl. Chem.*, **33**, 317 (1973).

Qualitative Potential Energy Surfaces. 4. Aromatic Substitution

N. D. Epiotis* and S. Shaik

Contribution from the Department of Chemistry, University of Washington, Seattle, Washington 98195. Received January 13, 1977

Abstract: Qualitative potential energy surfaces for electrophilic, photoelectrophilic, nucleophilic, and photonucleophilic aromatic substitutions are constructed and selection rules are derived. It is predicted that the regiochemistry of electrophilic and photonucleophilic aromatic substitutions is controlled by the electron density of the highest occupied MO of the aromatic substrate. On the other hand, the regiochemistry of nucleophilic and photoelectrophilic aromatic substitutions is controlled by the electron density of the lowest unoccupied MO of the aromatic substrate. The dependence of reaction rate and selectivity on polarity is discussed.

In a previous paper,¹ we outlined a qualitative theoretical method for constructing one-dimensional potential energy (PE) surfaces. We now use this approach in order to derive selection rules for the regiochemistry of thermal and photochemical nucleophilic and electrophilic aromatic substitutions.

I. Theory

A. Singlet Electrophilic Aromatic Substitutions. Consider the reaction shown below, where AY is an aromatic substrate, EX is an electrophile, and (AY-E)⁺ is the Wheland intermediate.²



The zero-order basis set configurations which are necessary for describing the addition step of the reaction sequence shown above along with the associated interaction matrix are shown in Scheme I, where AY is assumed to be the donor D and the

Scheme I. Zero-Order Basis Set Configurations and Interaction Matrix for Electrophilic Aromatic Substitutions

LU ^D	—	—LU ^A	—	+	+	—
HO ^D	+	+	+	+	+	—
	D	A	D ⁺	A ⁻	D [*]	A
		DA	D ⁺ A ⁻	D [*] A		
	DA	—	HO ^D -LU ^A	O		
	D ⁺ A ⁻		—	LU ^A -LU ^D		
	D [*] A			—		

electrophile E⁺X⁻ the acceptor A. The equations of the corresponding diabatic surfaces are given below and the diabatic as well as adiabatic surfaces are sketched in Figure 1. The meanings of the various symbols of eq 1-3 have been discussed in previous papers.¹

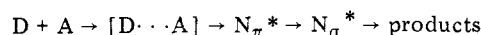
$$E(\text{DA}) = S(r) \quad (1)$$

$$E(\text{D}^+\text{A}^-) = I_D - A_A + S'(r) - C(r) \quad (2)$$

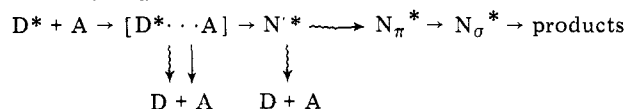
$$E(\text{D}^*\text{A}) = G(\pi\pi^*) + S'(r) \quad (3)$$

The information contained in the adiabatic potential surfaces can be conveyed by means of the chemical equations given below:

Thermal:



Photochemical:



The ground PE surface exhibits two barriers, E_A and E_B , and two intermediates, N_π^* and N_σ^* , both of which are described by a wave function with major charge transfer contribution. On the other hand, the first excited surface exhibits a barrier E^* followed by an excited intermediate N^* arising from the avoided crossing of the D^+A^- and DA diabatic surfaces. This intermediate can decay across the energy gap, ΔQ , and find its way to the ground-state surface. Hereafter, the reaction will take place on the ground surface, and hence its outcome will be determined partly by the properties of this surface.

In the case of the thermal reaction, it is clear that two different situations obtain depending on the relative sizes of the E_A and E_B barriers:

(a) Situations where $E_A > E_B$, i.e., reactions in which formation of N_π^* is rate controlling. These will be referred to as type A reactions.

(b) Situations where $E_A < E_B$, i.e., reactions in which formation of N_σ^* is rate controlling. These will be referred to as type B reactions.

On the other hand, the photochemical reaction is initiated on the lowest adiabatic excited surface, but it is completed on the ground surface. Accordingly, it is impossible to decide in